

Prediction of panellists' perception of bread crumb appearance using fractal and visual textural features

Ursula Gonzales-Barron · Francis Butler

Received: 6 November 2006 / Revised: 17 January 2007 / Accepted: 31 January 2007 / Published online: 1 March 2007
© Springer-Verlag 2007

Abstract Ratings of visual characteristics of bread crumb images obtained by panellists were correlated with features obtained by digital fractal and texture analysis and simple thresholding. Trained panellists were asked to rate 168 bread crumb images on fineness, homogeneity and degree of orientation, using continuous line scales. The relative orientation of the main and secondary peaks of the image power spectrum was the only parameter related to the human perception of the degree of crumb orientation. Single fractal dimension terms correlated better with the panellists' perception of grain fineness and homogeneity than the single crumb features from thresholding. Second-order polynomial models were significantly better ($P < 0.01$) in most predictors than simple linear models. Grain fineness was better approached by the method of relative differential box-counting fractal dimension ($R^2 = 0.822$) whereas grain homogeneity was highly related to the mass fractal dimension ($R^2 = 0.820$). Multiple linear models to estimate grain fineness with higher predictive capacity included predictors such as fractal dimension, mean intercellular distance and void fraction ($R^2 > 0.860$).

Keywords Bread crumb · Grain · Fractal dimension · Coarseness · Homogeneity · Orientation · Panellists

Introduction

Several studies ([1–3], among others) have shown that the development of an objective method to assess bread crumb grain properties using image processing techniques is useful not only from the point of view of quality assessment but also for studies concerning structural and mechanical properties [4–6]. For studies embracing bread crumb acceptance or preference by consumers, it is particularly desirable that the features obtained from image analysis are able to reflect panellists' ratings of bread crumb quality.

In this sense, a number of researches have attempted to predict panellists' ratings of bread crumb visual texture from image features. Zayas [7] extracted textural features from co-occurrence matrices along with shape and size measurements of the bread slices. The correlation of expert visual scores with image features was not very high ($R \sim 0.5$) in spite of statistical significances. Wang and Coles [8] employed both the fast Fourier transform and segmentation analysis to obtain features that could be related to experienced judges' scores. They awarded higher scores to finer textures and ignored occasional very large bubbles in sub-images. The power spectrum was calculated after a pre-processing series of band-pass filtering on the Gaussian masked bread image and generated textural features that correlated well with the expert score ($R^2 < 0.77$). The image segmentation was based on region growing from the estimated centres of gravity of the particles. The pore area and standard deviation gave better prediction of visual texture score ($R^2 < 0.84$). Day and Rogers [9] and Rogers et al. [3] utilised the frequency domain of sub-images of bread slices. They calculated composite results of fineness and elongation by

U. Gonzales-Barron (✉) · F. Butler
Biosystems Engineering, School of Agriculture,
Food Science and Veterinary Medicine,
University College Dublin, Earlsfort Terrace,
Dublin 2, Ireland
e-mail: ursula.gonzalesbarron@ucd.ie

computing the power spectral density of the Fourier transform and stacking the magnitudes of the transform from each sub-image. The composite spectrum was thresholded and an elliptical curve was fit by using Fourier descriptors. The fineness and elongation composite estimates derived from the ellipse correlated well to the experts' scores ($R^2 < 0.79$).

On the other hand, fractal dimension has been shown to be a highly accurate measure that presents strong correlation with human judgement of smoothness versus roughness of surfaces [10, 11]. Field [12] explained that many natural textures have a linear log power spectrum (which is related to fractal dimension), and that the processing in the human visual system is well suited to characterise such textures. Liu et al. [6] related the fractal dimension for cell numbers and fractal dimension for cell wall area to the elastic modulus of hydrated starch foam. Fractal texture analysis [13] has been successfully applied to characterise bread crumb grain in terms of crumb fineness, crumb homogeneity, cell wall tortuosity and interface ruggedness of cell–cell wall. However, the fractal dimensions have not been assessed with regard to their ability to correlate with sensory panellists' scores of crumb grain visual appearance. Therefore, the objective of this work was to assess the suitability of several fractal dimensions and orientation-related features (extracted from the Fourier power spectrum) in comparison with crumb features from thresholding to predict crumb grain attributes of fineness, homogeneity and orientation visually rated by trained panellists.

Materials and methods

Image acquisition and panellists' visual evaluation

One hundred and sixty eight bread crumb images presenting a wide range of fineness—coarseness, homogeneity—heterogeneity and degree of orientation were chosen from the images acquired by Gonzales-Barron and Butler [13]. Details of how the images were acquired are given in Gonzales-Barron and Butler [13].

A panel of ten assessors was trained in descriptive analysis of bread crumb grain images. During training, the panellists were first acquainted with the meaning of the visual descriptors selected, and then with the use of continuous scales with reference standards. They were exposed to a series of bread crumb images on which they were asked to agree on the score for each descriptor. Sets of 14 images were evaluated per session and assigned randomly to the panellists in different sessions so that all the results were the average of

five replicates. Continuous scales were employed to record the visual sensory ratings of the images on the following descriptors:

1. Fineness: related to visual estimation of the amount of gas cells; the continuous scale presented eight equally-spaced points. The reference standards from coarsest to finest grain of the Porentabelle scale [14] were anchored to each point over the scale;
2. Degree of homogeneity: which refers to the degree of uniformity of the pore sizes. This attribute was rated on a continuous category scale with the following unipolar intensity adjectives: 1 = poorly, 2 = slightly, 3 = moderately, 4 = very and, 5 = highly uniform; and,
3. Orientation: the degree of orientation of the crumb grain was rated on continuous category scale containing the words: 1 = not oriented, 2 = moderately oriented and 3 = very oriented. For both degree of uniformity and orientation, reference standard images were attached to the extremes of the scales [15].

Because the descriptive visual analysis was performed on images of the slices rather than on the original slices, biases due to differences in image properties were avoided. Thus, the difference in tonality and contrast between images were eliminated by setting the grey level mean to 140 (grey level scale) and equalising the histogram of all images. In addition, all the panellists' assessments were carried out using the same PC and under the same light conditions.

Image features from thresholding and fractal methods

To determine crumb features from thresholding, the images were binarised (converted from grey-level to black and white) using an automated fuzzy measure method [16]. One-pixel and two-pixel objects were cleaned out by an opening operation (erosion and dilation) with a two-row two-column structuring element of ones and small void areas within pores were filled. The following crumb features were obtained: (1) number of cells (Nc), (2) mean cell area in mm² (MCA), the average of all cells areas present in the crumb image, (3) standard deviation of cell areas in mm² (stCA), (4) void fraction (VF), defined as the fraction of the total area corresponding to the cells in the cut surface bread crumb, (5) mean intercellular distance in mm (ICD), defined as the average of the distances between cells at 0°, 45°, 90° and 135° of orientation [15], and (6) cell size uniformity (CSU),

defined as the ratio number of cells lower than 5 mm² to number of cells higher than 5 mm² were computed.

The fractal dimensions were obtained from the fractional Brownian motion method (FBM), the transform method (FFT), the relative differential box-counting method (RDBC), the morphological method (M), the mass fractal method (MF) and the random walks method (RW), following the equations outlined in Gonzales-Barron and Butler [13].

Image texture and orientation features

The following features were extracted from the Fourier power spectrum of the images:

- (a) Radial distribution of the Fourier power spectrum. The discrete Fourier transform of an image $I(x,y)$ is defined by

$$F(u, v) = \frac{1}{M^2} \sum_{x,y=0}^{M-1} I(x, y) e^{-2\pi\sqrt{-1}(ux+vy)}$$

and the Fourier power spectrum is $|F|^2 = FF^*$, where * denotes the complex conjugate. It is well known that the radial distribution of values in $F(u,v)$ is sensitive to texture coarseness in $I(x,y)$ [17]. A coarse texture will have high values of $F(u,v)$ concentrated near the origin, while in a fine texture, the values of $F(u,v)$ will be more spread out. Thus, a set of useful energy features are the averages of $F(u,v)$ taken over ring-shaped regions (E_{ring}) centred at the origin for various values of r , the ring radius.

$$E_{ring\ r_1 r_2} = \sum_{r_1}^{r_2} F(u, v), \quad r_1^2 \leq u^2 + v^2 < r_2^2, \\ 0 \leq u, \quad v \leq n - 1$$

- (b) Angular distribution of the Fourier power spectrum

The angular distribution of values in the power spectrum is sensitive to the directionality of the texture in I . If a texture is oriented in given direction θ , it will have high values of $|F|^2$ concentrated around the perpendicular direction $\theta+(\pi/2)$ [17]. Thus, a set of energy features (E_{wedge}) for analysing texture directionality will be taken over wedge-shaped regions by using,

$$E_{wedge\ \theta_1 \theta_2} = \sum_{\theta_1}^{\theta_2} F(u, v), \quad \theta_1 \leq \tan^{-1}(v/u) < \theta_2, \\ 0 \leq u, \quad v \leq n - 1$$

The ring-shaped regions were computed for the radii $[r_1, r_2] = [2, 4], [4, 8], [8, 16], [16, 32]$ and $[32, 64]$; and the wedge-shaped regions for the angles $[\theta_1, \theta_2] = [-22.5, 22.5], [22.5, 67.5], [67.5, 112.5], [112.5, 157.5]$. Also, all possible intersections of rings and wedges were computed.

- (c) Orientation of major and secondary peaks. Liu and Jernigan [18] defined a set of 28 frequency domain features for texture discrimination in additive noise from which the major and secondary peaks orientations were utilised. The frequency coordinates of the maximum peak (u_1, v_1) and second largest peak (u_2, v_2) of the power spectrum $F(u,v)$ were found and their orientation computed as $\tan^{-1}(v_1/u_1)$ and $\tan^{-1}(v_2/u_2)$, respectively.

The fuzzy thresholding method, the crumb features from thresholding, the fractal methods, and the image orientation features were written in Matlab 6.12 (The MathWorks Inc., Natick, MA, USA).

Statistical evaluation

An incomplete block experimental design was devised for the three descriptors used. Sets of 14 images were evaluated per session and assigned randomly to the panellists in different sessions so that all the results were the average of five replicates. Analysis of variance of linear and second-order regressions with their respective coefficient of determination (R^2) between all possible pairs of a visual sensory property and an image feature was computed. The stepwise regression option (sle and sls = 0.15) of SAS (version 8.2, SAS Institute Inc, NC, USA) was used to select the best predictors of the panellists' sensory responses from all the image textural features in order to build multiple regression models. Comparisons between nested models were performed using the F -test according to Mendenhall and Sincich [19].

Results and discussion

Table 1 shows the coefficients of determination for the regressions of the panellists' perception of grain fineness and homogeneity with the crumb features from thresholding and the fractal dimensions. From the crumb features, ICD and Nc exhibited the highest coefficients of determination with grain fineness ($R^2 = 0.785$ and 0.725 , respectively, in Table 1). It is clear that as the number of cells increases, the distance between gas cells becomes smaller and the grain is

Table 1 Coefficients of determination of the regression models ($p < 0.05$) of grain fineness and homogeneity from panellists' scores with image features: crumb features from thresholding and fractal dimensions

Independent variables		R^2_{adj} for fineness	R^2_{adj} for homogeneity
Crumb features from thresholding			
1	Nc	0.699	0.483
2	Nc, Nc ²	0.725	0.505
3	MCA*	0.657	0.455
4	sdCA	0.638	0.654
5	sdCA, sdCA ²	0.644	0.677
6	ICD*	0.785	0.650
7	CSU	0.450	0.274
8	CSU, CSU ²	0.534	0.327
Crumb fractal dimensions			
9	RDBC	0.783	0.660
10	RDBC, RDBC ²	0.822	0.688
11	FBM	0.525	0.341
12	FBM, FBM ²	0.545	0.351
13	FFT	0.690	0.582
14	FFT, FFT ²	0.713	0.601
15	MF	0.705	0.764
16	MF, MF ²	0.766	0.820
17	Rw*	0.384	0.252
18	M*	0.187	0.116

* Coefficient of determination of this linear regression was higher than that of its second order polynomial

finer. In most crumb features, the second-order polynomial models (Table 1) presented a higher R^2 for grain fineness and homogeneity than their counterpart linear models.

From the fractal dimension, the RDBC method displayed the best correlation to grain fineness ($R^2 = 0.822$). Thus, the RDBC method was found to be a better predictor of fineness than the crumb grain features obtained by thresholding (ICD, Nc). For grain homogeneity, sdCA and ICD were the crumb features that showed the highest coefficients of determination ($R^2 = 0.677$ and 0.650). However, the fractal dimension from the MF method correlated very well with grain homogeneity and its coefficient of determination (0.820) was much higher than the ones with sdCA and ICD. Again for the fractal dimensions, the second-order polynomial models showed in Table 1 presented the higher R^2 for grain fineness and homogeneity. The prediction of grain fineness and homogeneity as perceived by panellists fitted polynomial models (Figs. 1, 2) because the human perception of sensory signals is thought to involve non-linear processing of sensory information by a massive network of neurons [20]. Excepting for MCA, ICD, Rw and M, all the polynomial models in Table 1 were found statistically better in predictive terms ($P < 0.01$) than their respective simple linear models. Consequently, the fractal

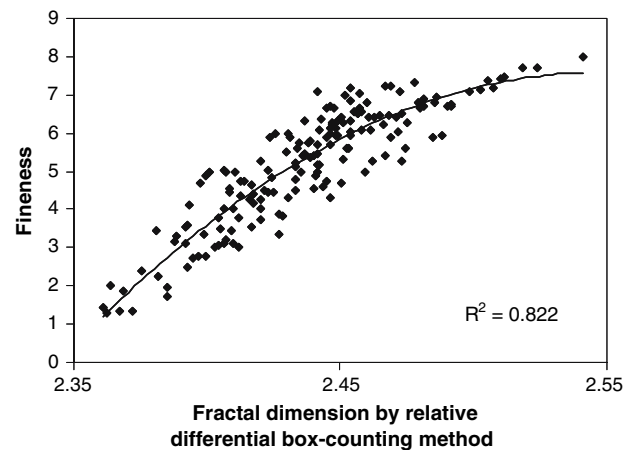


Fig. 1 Fineness of bread crumb grain related to fractal dimension estimated from the relative differential box-counting method

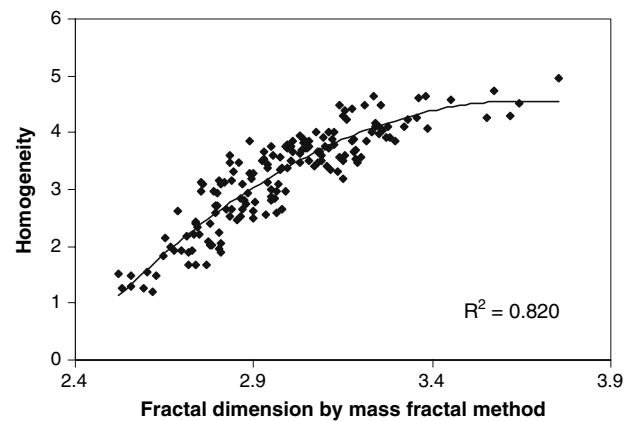


Fig. 2 Homogeneity of bread crumb grain related to fractal dimension estimated from the mass fractal method

dimensions provided better approximation to the human perception of grain fineness and homogeneity than the crumb features extracted from thresholding.

There was sizeable interdependence between many of the visual and the crumb grain features. Grain fineness and homogeneity were found to be linked properties ($R^2 = 0.6230$). Fineness is related mainly to the cell size while the homogeneity is related to cell size variability. However, mean cell size and its variability were also related parameters. As the cell size increased, the standard deviation increased as well, as shown in Fig. 3, which displays the second-order polynomial relationship ($R^2 = 0.669$).

Models for predicting the grain fineness and homogeneity were developed using stepwise regression analysis. All variables: crumb features, fractal dimensions and Fourier power spectrum features were considered. For grain fineness, the significant predictors

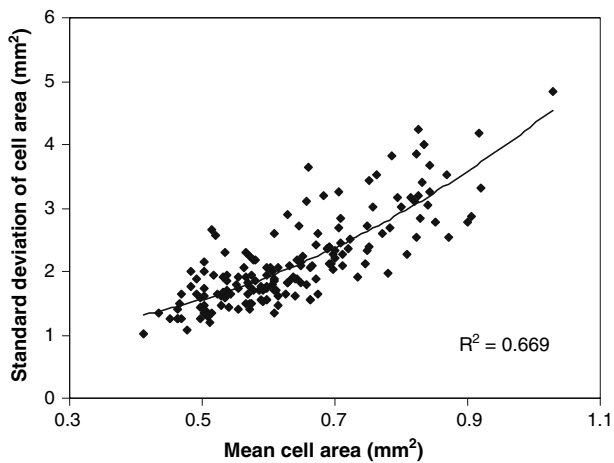


Fig. 3 Relationship between mean cell area and cell area standard deviation for the images analysed

were RDBC fractal dimension, mean intercellular distance, void fraction, energy of power spectrum, morphological fractal dimension and random walks fractal dimension (Table 2). The term RDBC squared was not selected by the stepwise analysis, but model 1 in Table 2 was included for comparison as the relationship between fineness and FD was non-linear (Fig. 1). Models 2, 3, 4 and 5 added one predictor at a time to the previous equation so that the predictive capacity of the new model was improved significantly ($P < 0.01$). The variables selected by the stepwise selection for predicting grain homogeneity were mass fractal dimension, squared mass fractal dimension, squared fast-Fourier-transform fractal dimension and energy of power spectrum. Likewise, models 7 and 8

Table 2 Multiple regression models that best predict panellists' scores of grain fineness and homogeneity selected by stepwise regression analysis

Regression models	R^2_{adj}
Fineness (F)	
1 $F = -1185 + 936 \text{ RDBC} - 184 \text{ RDBC}^2$	0.822
2 $F = -38.2 + 20.3 \text{ RDBC} - 0.0304 \text{ ICD}$	0.821
3 $F = 0.48 + 10.3 \text{ RDBC} - 0.0509 \text{ ICD} - 24.7 \text{ VF}$	0.864
4 $F = 7.42 + 8.23 \text{ RDBC} - 0.0519 \text{ ICD} - 27.3 \text{ VF} - 3.14 \text{ E}_{ring4-8}$	0.874
5 $F = -10.6 + 12.6 \text{ RDBC} - 0.050 \text{ ICD} - 23.1 \text{ VF} - 3.29 \text{ E}_{ring4-8} + 2.33 \text{ M}$	0.884
6 $F = -11.6 + 13.5 \text{ RDBC} - 0.046 \text{ ICD} - 22.7 \text{ VF} - 3.43 \text{ E}_{ring4-8} + 3.28 \text{ M} - 1.57 \text{ RW}^2$	0.886
Homogeneity (H)	
7 $H = -31.01 + 19.46 \text{ MF} - 2.66 \text{ MF}^2$	0.820
8 $H = -34.7 + 19.0 \text{ MF} - 2.65 \text{ MF}^2 + 0.733 \text{ FFT}^2$	0.826
9 $H = -36.4 + 20.2 \text{ MF} - 2.88 \text{ MF}^2 + 0.769 \text{ FFT}^2 - 1.24 \text{ E}_{ring4-8}$	0.830

inserted one significant predictor. The energy of the power spectrum in the ring from frequencies 4 to 8 ($E_{ring4-8}$) was selected as a variable for predicting both grain fineness and homogeneity because the radial distribution of values of the power spectrum is sensitive to texture coarseness. To estimate fineness and homogeneity, models 3 and 7 provided a good trade-off between predictive capacity and number of terms.

Grain orientation was not linked to any crumb features extracted by thresholding or the fractal dimensions. Bread crumb isotropy, a parameter related to cell shape and orientation [15], is not determined either by grain coarseness (coefficient of correlation of 0.324 [15]) or by grain heterogeneity (coefficient of correlation of 0.333 [15]). The results of the power spectrum wedges indicated that 68% of the images rated by the panellists as not—slightly oriented (1.0–1.5 on the continuous scale) presented higher energies in the wedges of the spectrum with centres 0° and 90° (i.e., x and y axes). However, none of the power spectrum wedges correlated with the panellists' scores of crumb orientation.

Figure 4 is a plot of Liu's features, major and secondary peak orientations, showing the contours of the orientation intensities in the intervals [1 1.5], <1.5 2], <2 2.5] and <2.5 3]. Two main clusters were observed for the images rated between moderately and highly oriented (2.0–3.0 on the continuous scale). The first cluster A (Fig. 4) lies between the major peak angle range of $[45^\circ 100^\circ]$ and the secondary peak angle range of $[130^\circ 160^\circ]$ and contains 60% of the images rated in this interval. The second cluster B is positioned between the main peak angle range of $[110^\circ 155^\circ]$ and

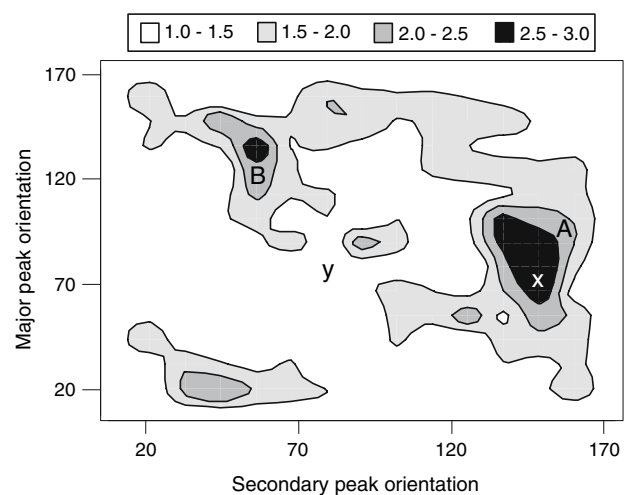
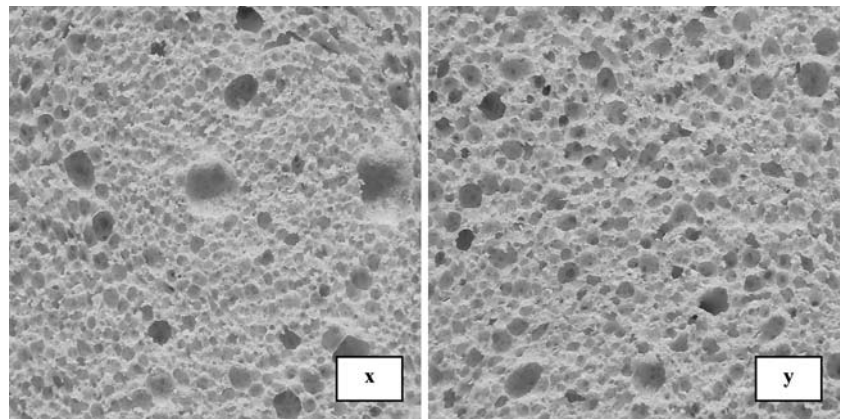


Fig. 4 Contours plot of intervals of bread crumb orientation [1.0 1.5], <1.5 2.0], <2.0 2.5], <2.5 3.0] as perceived by panellists as a function of the major and secondary peaks orientation of the Fourier power spectrum

Fig. 5 Two bread-crumb samples with different degree of orientation. Panellists' mean scores were 2.55 and 1.10 for samples *x* and *y* (1 not orientated, 3 very orientated)



secondary peak angle range of $[35^\circ\ 60^\circ]$ and contains 28% of the images perceived as moderately to very oriented. To explain the occurrence of these clusters, Fig. 5 shows an example of two bread crumb samples with different degree of orientation. Sample *x* has a more oriented texture compared to Sample *y*. For sample *x* (position *x* in Fig. 4), the orientations of main and secondary peaks were 75.0° and 135.0° . While for sample *y*, those values were 75.9° and 84.3° , respectively (position *y*). This implies that when the orientation of the main and secondary peaks of the power spectrum is considerably different, the bread crumb image tends to be observed as moderately—highly oriented due to the existence of either at least two directions of orientation or a curly textured pattern. This would explain the presence of the two main clusters A and B. Nonetheless, some textures having their peaks located at nearby orientations around 20° – 45° were detected as moderately oriented in one direction (bread crumb orientation $<2.0\ 2.5$). This can be distinguished in the small island near the origin in Fig. 4. However, no equations to predict the panellists' perception of image orientation from the Fourier power spectrum could be modelled considering the non-continuous nature of the data distribution.

Conclusions

The high coefficient of determination between fractal dimension and visual appearance of the bread-crumbs images clearly validates the usefulness of the fractal approach for the study of the bread crumb quality assessment. The panellists' visual scores of grain fineness and homogeneity could be predicted by second-order polynomial models of the fractal dimensions obtained with the relative differential box-counting method and the mass fractal method, respectively, with

coefficients of determination of 0.82. Regarding the crumb features obtained by image thresholding, grain fineness showed high correlation to both mean inter-cellular distance and number of cells, and grain homogeneity correlated well with the standard deviation of cell areas, although the fractal dimensions adjusted better to the panellists' perception of these properties than did the crumb features extracted by thresholding. However, multiple models, developed with stepwise regression, could attain coefficients of determination higher than 0.82. A significantly-improved model to predict grain fineness including terms such as fractal dimension, mean inter cell area, void fraction and a measure of power spectrum energy achieved a coefficient of determination of 0.87. Finally, no model to predict the degree of orientation of the grain could be ascertained from the textural features used here; although results showed that relative orientation of the main and secondary peaks of the power spectrum was related to the human perception of the image orientation. Images, whose relative orientation of peaks of power spectra was high, were mostly perceived as moderately to highly orientated. Other orientation features should be investigated in order to predict the degree of orientation perceived by panellists.

Acknowledgments The Authors wish to acknowledge that this work was funded by the Irish Department of Agriculture through the Food Institutional Research Measure.

References

- Bertrand D, Le Guenverve C, Marion D, Devaux M, Robert P (1992) *Cereal Chem* 69:257–261
- Sapirstein HD, Roller R, Bushuk W (1994) *Cereal Chem* 71(4):383–391
- Rogers DE, Day DD, Olewnik MC (1995) *Cereal Foods World* 40(7):498–501

4. Zghal MC, Scanlon MG, Sapirstein H (1999) *Cereal Chem* 76:734–742
5. Zghal MC, Scanlon MG, Sapirstein HD (2002) *J Cereal Sci* 36:167–176
6. Liu Z, Chuah CSL, Scanlon MG (2003) *Act Mater* 51:365–371
7. Zayas IY, Steele JL, Weaver G, Walker DE (1993) *SPIE Proc Mach Vis Archit Integr Appl* 2064:135–151
8. Wang J, Coles GD (1993) Image processing methods for determining bread texture. In: *Proceedings of the first New Zealand conference on image and vision computing*, Auckland, pp 125–132
9. Day DD, Rogers D (1996) *Digit Signal Proc* 6:138–144
10. Pentland A (1984) *IEEE Trans PAMI* 6:661–674
11. Chaudhuri BB, Sarkar N (1995) *IEEE Trans PAMI* 17(1):72–77
12. Field DJ (1987) *J Opt Soc Am A* 4:2379–2394
13. Gonzales-Barron U, Butler F (2007) Fractal texture analysis of bread crumb digital images. *Eur Food Res Tech*. doi:10.1007/s00217-007-0582-3
14. Dallman H (1969) *Porentabelle*. Verlag Moritz Schäfer, Detmold
15. Gonzales-Barron U (2006) Quantitative assessment of bread crumb quality using image analysis. PhD Thesis, University College Dublin, Department of Biosystems Engineering, Dublin, Ireland
16. Huang LK, Wang MJ (1995) *Pattern Recog* 21(1):41–51
17. Weszka JS, Dyer CR, Rosenfeld A (1976) *IEEE Trans Syst Man Cybern* 6(4):269–285
18. Liu SS, Jernigan ME (1990) *Comput Vis Graph Image Proc* 49:52–67
19. Mendenhall W, Sincich T (1995) *Statistics for engineering and the sciences*, 4th edn. Prentice Hall, Englewood Cliffs
20. Gao X, Tan J, Shatadal P, Heymann H (1999) *J Texture Stud* 30:291–304